Acquiring physically-modeled seismic data using 70kHz piezoelectric buzzers

Wong, J., Bertram, K. L., and Innanen, K. A. H.

ABSTRACT

Efficient full-waveform inversion (FWI) imaging of complex velocity structures requires seismic data with low dominant frequencies in the range of 4Hz to 10Hz. When immersed in water in the laboratory, piezoelectric buzzers on will generate and detect vibrations with low-end ultrasonic frequencies ranging from 40kHz to 100kHz, so physically-modelled seismograms recorded with buzzer transducers will have the low frequencies (after applying a scaling factor of 10^4) required for seismic FWI. However, due to resonance effects in the buzzers, the seismogram codas are too long and too variable for them to serve as ideal FWT source wavelets. Finding ways to mitigate these two unfavorable characteristics is an ongoing task in our research in physical modelling.

INTRODUCTION

Full-waveform inversion (FWI) applied to seismic data has the ability to produce high-resolution images of complex geological velocity structures. Images produced by FWI generally have much higher resolution than images produced by migration methods. FWI is an iterative process that employs repeated numerical modelling of seismograms via finite difference or finite element algorithms.

FWI is promising but also suffers from many challenges, one of which is cycle-skipping. For successful application of FWI, numerically-modelled data must match the observed data at all usable frequencies within half a wave-cycle. With frequencies as high as 50Hz, repetitive finite difference modelling as the procedure searches for a velocity-density model to fit the observed data without cycle-skipping becomes very burdensome.

Theoretically, at low frequencies, there is a high chance that the modelled and observed data match within half a wave-cycle. Hence, low frequencies are crucial to recovering the long wavelength structures of the model (Sirgue and Pratt, 2004; Pan et al., 2015). Therefore, efficient application of the technique to realistic geological environments requires that the input seismic data have low dominant frequencies, typically in the range of about 4Hz to 10Hz. The seismograms must be digitized at fast enough sampling rates to accurately capture small phase changes in transmission and reflection arrivals so that geological features with dimension as small as 10m can be resolved. Sampling times of one or two milliseconds are adequate.

We used the University of Calgary Seismic Physical Modelling Facility (Wong et al., 2009) to produce seismic data with the (scaled) low frequencies needed for efficient FWI imaging algorithms. Physical scale modeling in the laboratory of real-world seismic surveys means that geological dimensions on the order of kilometers be reduced to tens of centimeters, and that seismic exploration sampling times of milliseconds be reduced to factions of microseconds. In the University of Calgary Seismic Physical Modelling Facility, we typically apply a scale factor of 10^4, so that 1m and 1ms in the seismic exploration world are represented by 0.1mm and 0.1μs in the laboratory.

In the past, we have used 2.36-mm-diameter piezopin transducers as sources and receivers for seismic physical modelling. Piezopins yield seismograms with scaled dominant frequencies of about 50Hz. In order to achieve dominant frequencies in the range 4Hz to 10Hz, we instead use piezoelectric buzzers as sources and receivers. We present physically-modelled seismograms acquired across a 2D circular plane acquired with these buzzers immersed in water.

METHOD

The specific transducers we used to produce the low-end ultrasonic frequencies are Murata PKM13EPYH4002-B0 piezoelectric buzzers (Figure 1). The buzzers have diameters of about 13mm and thicknesses of 6.9mm. We used a single buzzer as a source and a single buzzer as a receiver mounted on the Physical Modelling Positioning Subsystem. We immersed them in a homogeneous volume of water (acoustic velocity of 1485 m/s) and moved them independently to the desired source/receiver locations. Figure 2 shows the acquisition geometry used to acquire a set of transmission seismograms across a 2D circular plane with diameter of approximately 30cm (3000m scaled).

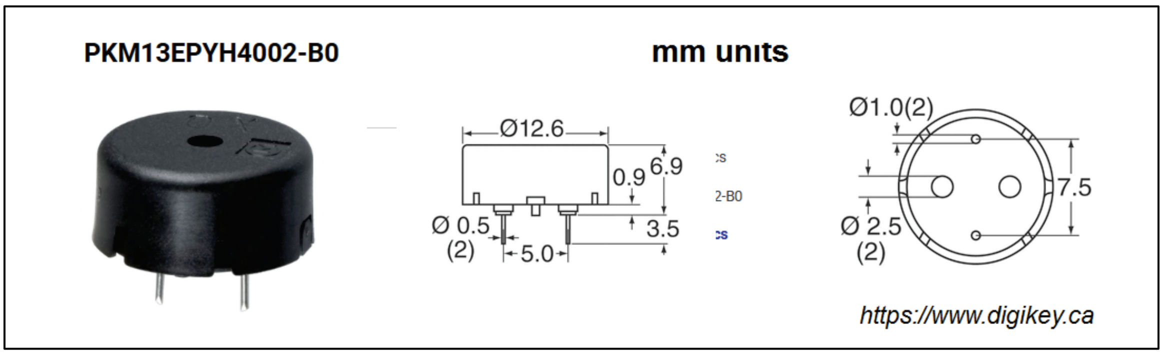

Fig. 1. Murata 13mm-diameter piezoelectric buzzer. When driven by a voltage impulse, act as a damped Helmholtz resonator generating relatively low ultrasonic frequency vibrations that emanate from the small port on its top face.

Limitations in acquisition geometry and scanning procedure

The positioning subsystem and the physical sizes of the 13mm-diameter buzzer transducers complicate the acquisition geometry used for physical modeling. To prevent the two positioning Gantries A and B from colliding, the X coordinate of Gantry A must always be less than the X coordinate of Gantry B. In addition, the 13mm-diameter source and receiver buzzer transducers must be moved and positioned so that they never hit each other. To ensure this for the present acquisition, the source on Gantry A and the receiver on Gantry B are always kept separated in the X coordinate by at least 400m (40mm unscaled).

This is achieved by initially assigning a position on the circumference of the circle for the source transducer and then -200m is added to its X coordinate. An initial position on the circumference is similarly assigned to the receiver transducer and then +200m is added to its X coordinate. The sequence of steps in moving the source and receiver transducers must be designed so that collisions will never happen.

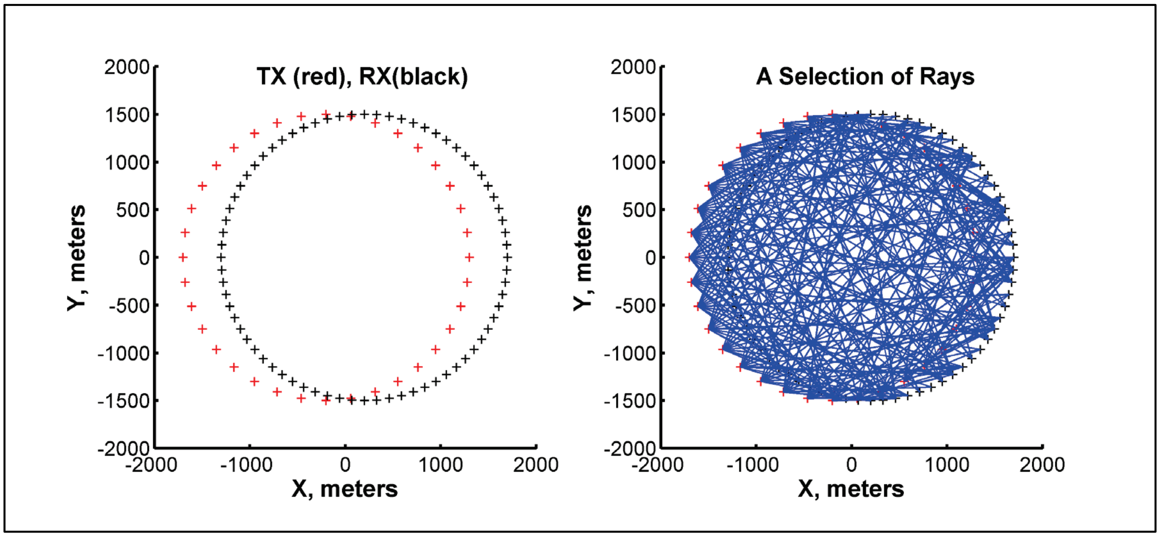

Fig. 2. Acquisition geometry. Left: Locations of sources and receivers marked by colored crosses. Right: Raypaths joining source s and receivers (only every fifth raypath is shown).

RESULTS

Seismograms were recorded in the homogeneous volume of water using the 2D acquisition geometry shown on Figure 2. The data were archived in the SEGY file **bzzr_No_Target_40db.sgy.** The file contains 37 common-source gathers (CSGs). Each CSG has 1, 5, 9, …69, 73, 69, …9, 5, or 1 seismograms, for a total of 1333 seismic traces. Each trace is 3072 samples long digitized at a scaled interval of 1ms. A recorded trace is the result of driving the source transducer with a 40V impulse-like signal, amplifying the received signal by 40dB, and stacking the amplified signal for 100 firings of the source. Scaled source-receiver XY coordinates are recorded in the SEGY trace headers in units of meters times 10.

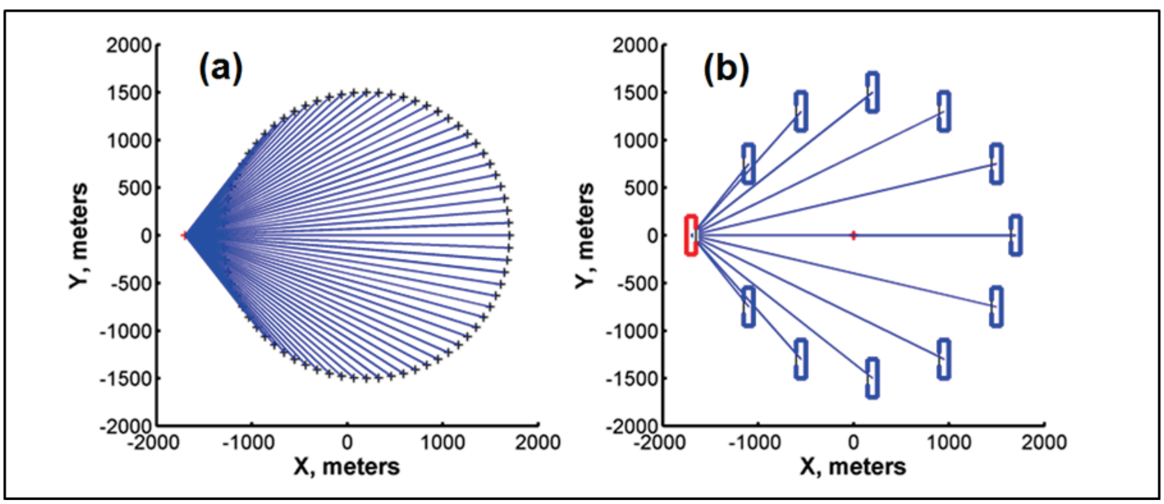

Fig. 3. (a) Raypaths for an example CSG from file bzzr_No_Target_40db.sgy (b) Schematic showing rectangular transducer footprints in the XY plane.

Figure 3(a) shows the raypaths for an example CSG selected from the dataset. For this CSG, the source is fixed at location (X=-1700m, Y=0m). The receiver locations fall on the circle circumference but are displaced by +200m in the X-coordinate. The maximum source-receiver separation for the figure is 3400m (scaled). Figure 4 shows the azimuth angles for the raypaths shown on Figure 3(a).

The transducer coordinates recorded on the SEGY tracer headers nominally refer to the center of the transducer ports on Figure 1. As is shown on Figure 3(b), the particular method used to mount the buzzers to the positioning system for the present acquisition results in rectangular transducer footprints in the XY plane. The transducers do not approximate 2D point sources and receivers at all. Consequently, we expect directional and asymmetric radiation and reception patterns to affect the acquired seismograms.

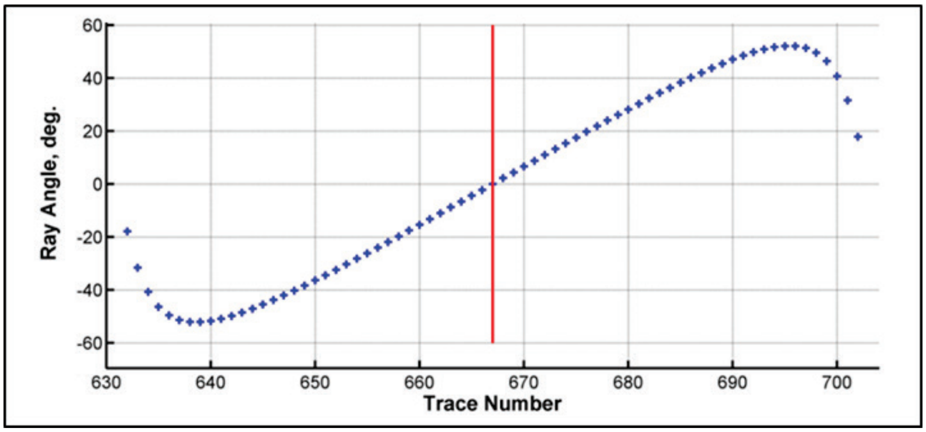

Fig. 4. Azimuth angles relative to the X-axis for the rays shown on Figure 3.

Figure 5 displays seismograms from the example CSG with each seismogram normalized by its maximum peak-to-peak amplitude. The first arrivals follow the trajectory of travel times calculated for the source-receiver positions. The traces have long-duration codas that change with every source-receiver position. The long durations exist because the buzzers act as under-damped Helmholtz resonators. The variation of trace waveforms with receiver position is caused by mismatches in the directional and asymmetric radiation/reception patterns. The variations are exacerbated by in-plane and out-of-plane scattering of the long signal durations by the buzzer bodies.

Figure 6 displays aligned normalized traces from the example CSG after frequency filtering. Since the data were acquired in a homogeneous medium, we can consider each trace to be a recording of the source/receiver wavelet. Summing the aligned traces yields the average trace displayed together with its power spectrum on Figure 7. The spectrum indicates that buzzers used as sources and receiver in water produce source wavelets with low frequencies (4Hz to 10Hz, scaled) energy sufficient for efficient FWI imaging. However, the codas of these “source” wavelets are too variable and too long to be optimal for efficient FWI algorithms. The problem of non-stationary long-duration source wavelets must be addressed before buzzers can be used in physical modelling to produce experimental acoustic data suitable for efficient FWI (Wong et al., this volume).

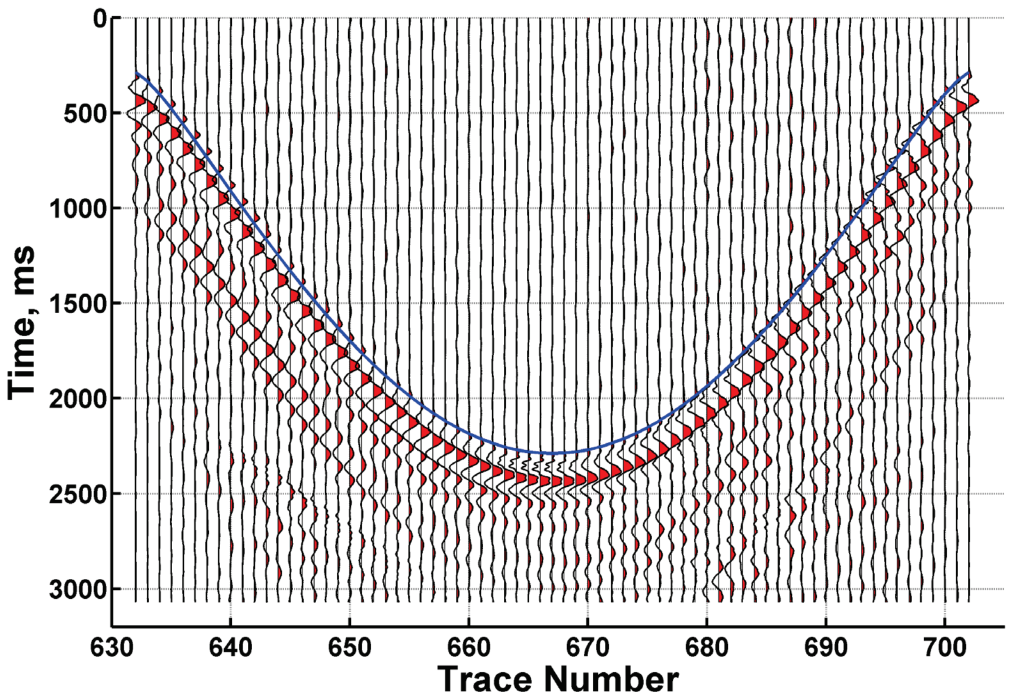

Fig. 5: Trace-normalized display of selected raw transmission seismograms through a homogeneous medium (water). Blue line marks the water arrival times. Note the long-duration codas and lack of symmetry with respect to the apex position (Trace Number 667).

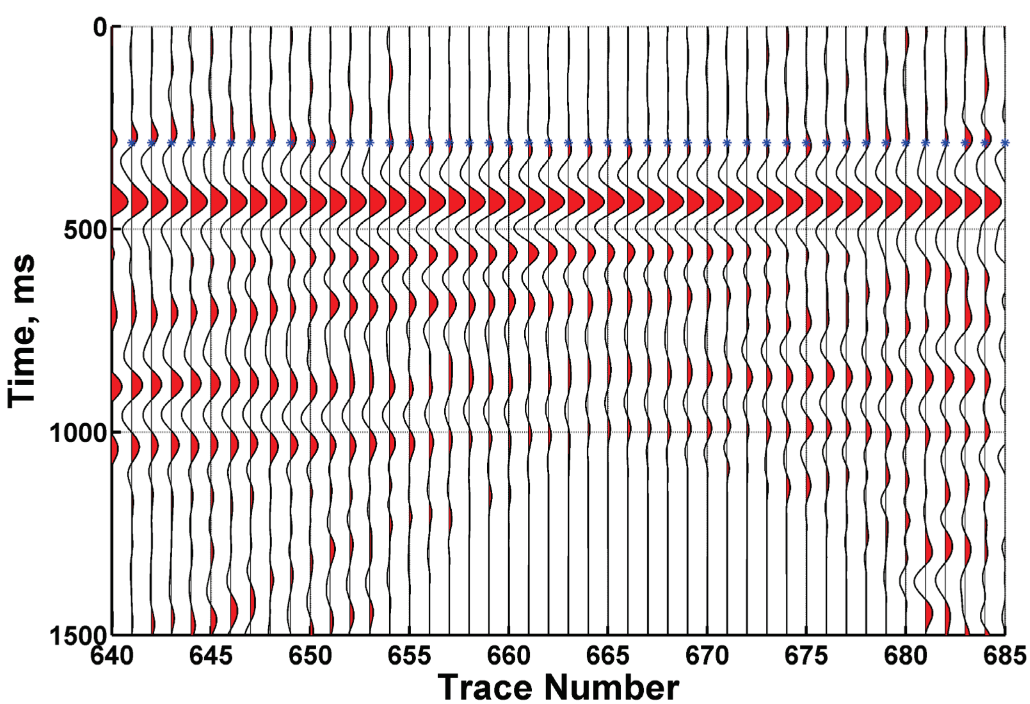

Fig. 6: Traces from Figure 5 aligned to water-arrival times, and then trimmed aligned to first-peak times. An Ormsby bandpass filter with parameters [0.2 1.0 10 20] Hz has been applied.

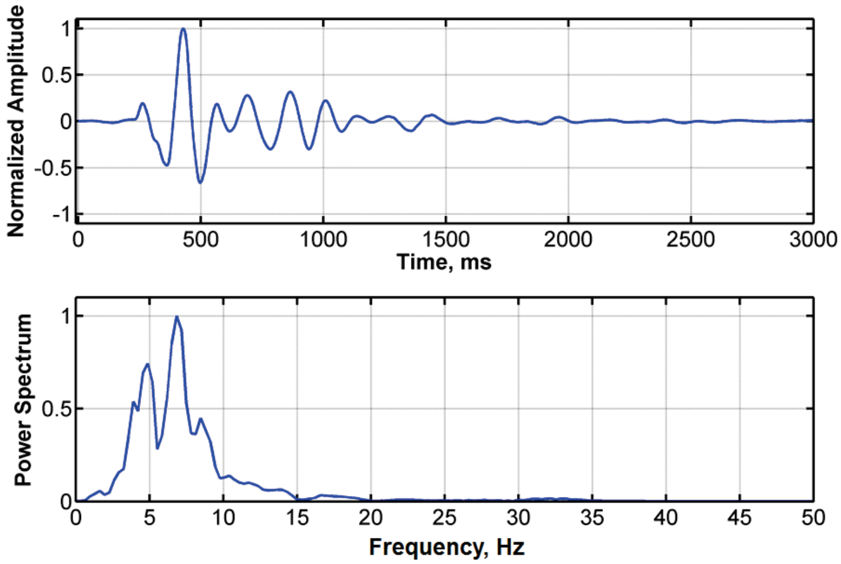

Fig. 7. Average of traces on Figure 6 and its spectrum.

TIME-LAPSE EXPERIMENT

We placed a solid PVC target within the circular area and repeated the acquisition with exactly the same source-receiver positioning as shown on Figure 2. The dataset was archived as **bzzr_PVCTarget_40db.sgy**. The files **bzzr_No_Target_40db.sgy** (baseline survey) and **bzzr_PVCTarget_40db.sgy** (monitor survey) can be considered as the results of simulated time-lapse seismic surveys.

Figure 8 is a plot of selected seismograms from the baseline survey; Figure 9 is a plot of selected seismograms from the monitor survey with the same source/receiver positions. Each plotted trace is the raw trace normalized by its maximum peak-to-peak amplitude with no additional processing. We see that the two plots appear to be almost identical, except for the traces just to the left of the apex position at trace number 667.

Figure 10 is a comparison plot of the true peak-to-peak amplitudes of the seismograms on Figures 8 and 9 as a function of trace position. Time-lapse repeatability of the physical modeling measurements is indicated by the nearly identical amplitudes for both sets of traces except close to the location of the PVC target (trace numbers 657 to 670).

Figure 11 is a plot of the difference traces obtained by subtracting the baseline traces (Figure 8) from the monitor traces (Figure 9). Figure 12 flattens the difference traces to the minimum water-arrival time shown on Figure 11. Travel-time and amplitude anomalies on both figures clearly indicate the presence and rough extent of the target. Back-projection of observed anomalies from 1333 traces would roughly define the location and size of the target within the scanned area (Henley, this volume).

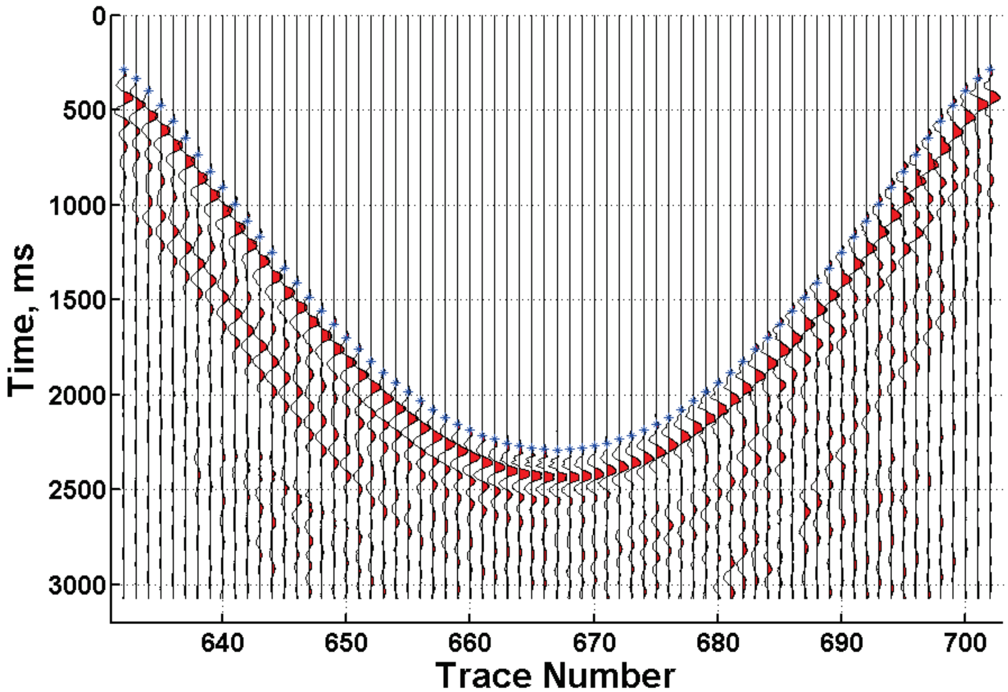

Fig. 8. Trace-normalized display of selected raw seismograms from the baseline survey. Blue crosses mark calculated first-arrival times through water. All trace values prior to the first-arrival times have been muted since they play no role in FWI. No other processing.

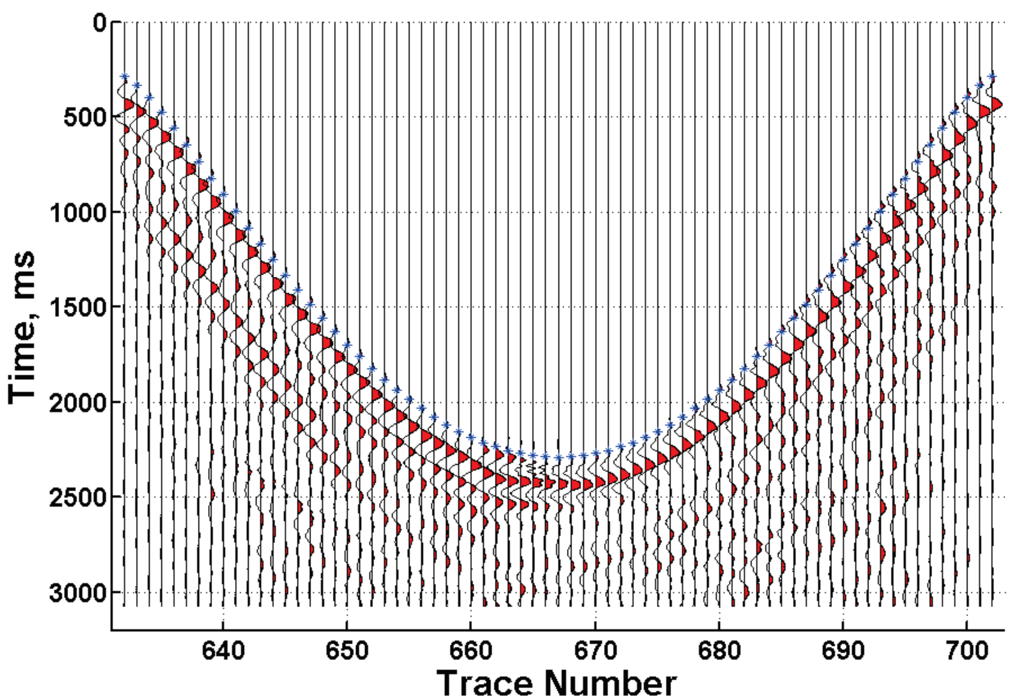

Fig. 9. Trace-normalized display of selected traces from the monitor survey. All trace values prior to the first-arrival times have been muted since they play no role in FWI. No other processing.

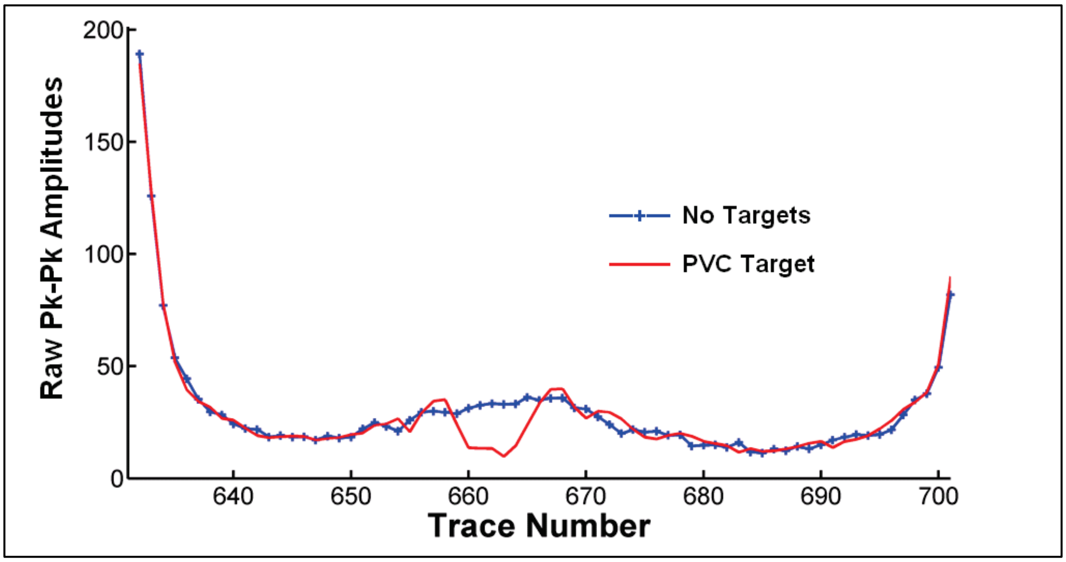

Fig. 10. True maximum peak-to-peak amplitudes of seismograms from the baseline and monitor surveys. Trace amplitudes are almost identical except for rays through the target.

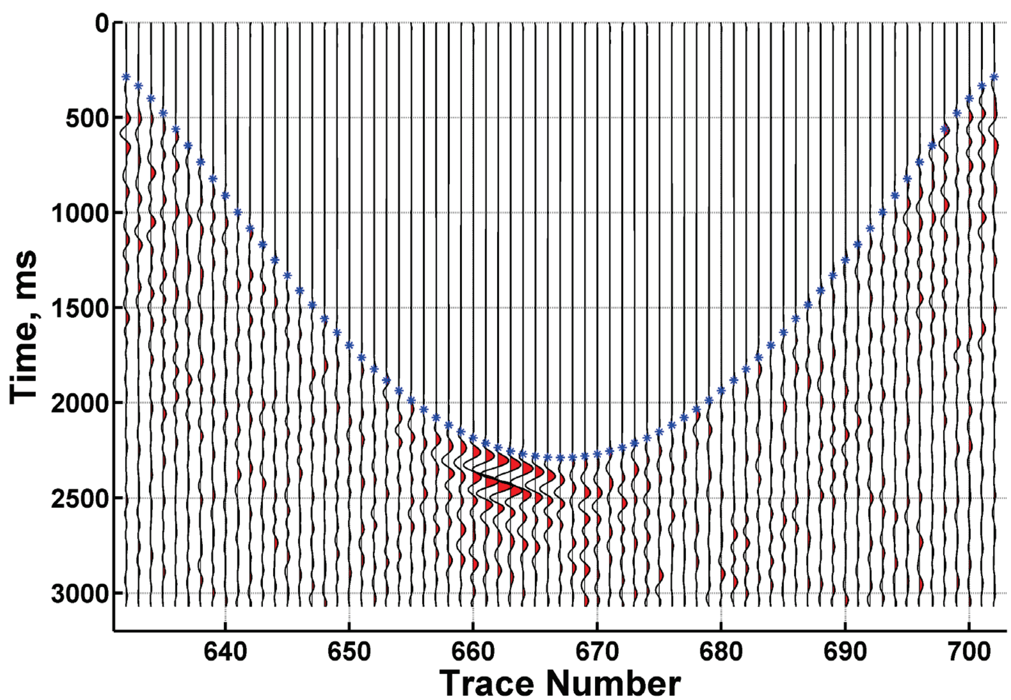

Fig. 11. Difference between raw traces from the monitor and baseline surveys, plotted after normalizing to highlight the anomaly. Frequency-filtered with Ormsby bandpass filter parameters of [0.2 1.0 10 20] Hz.

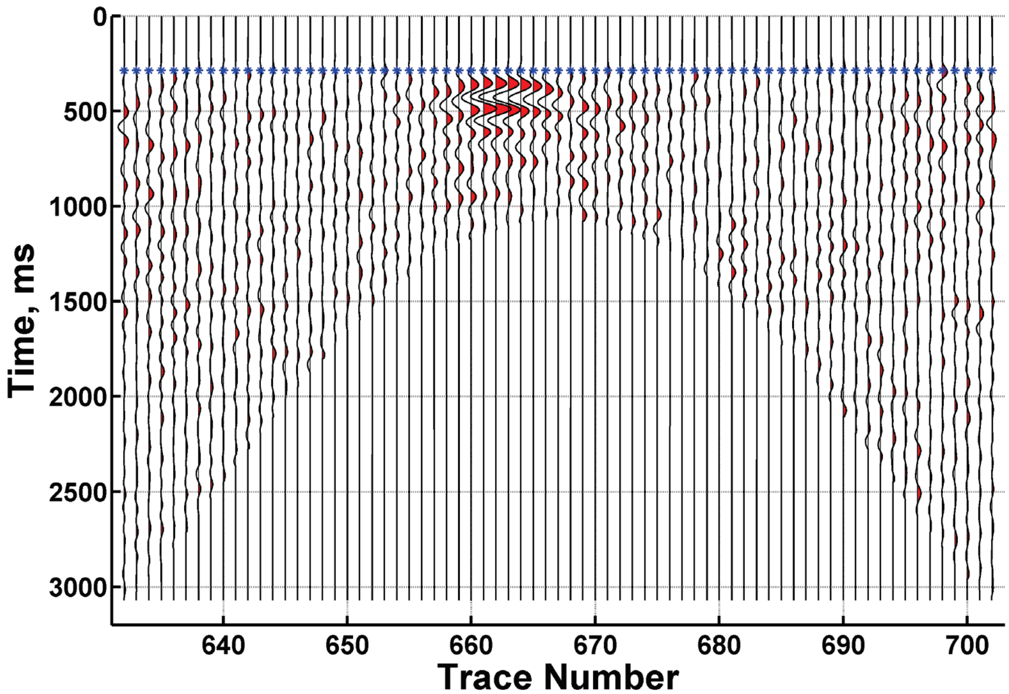

Fig. 12. Difference traces from Figure 11 aligned to the minimum water-arrival time on Figure 11.

SUMMARY AND DISCUSSION

Using 13mm-dtameter piezoelectric buzzers immersed in water as source and receiver in physical modelling seismic acquisition, we recorded seismic data with significant energy in the low-frequency range needed for efficient FWI. The buzzers act as Helmholtz resonators designed to produce relatively low ultrasonic frequencies. They generated and detected vibrations with laboratory frequencies ranging from 40kHz to 100 kHz that scale down to seismic-exploration frequencies of 4Hz to 10Hz. Laboratory dominant wavelengths are on the order of 15mm-38mm; these scale up to seismic-exploration wavelengths of 150m-380m. Under-damped resonance within the buzzers results in signals with several slowly-decaying cycles of the dominant frequency that appear long-duration signal codas.

As shown on Figures 3(b) and A1(a), the footprints of the source and receiver transducers in the XY plane are rectangular in shape due to the way they were mounted for the measurements in this report. The footprints are radially asymmetric and deviate from ideal point source-receiver geometries. The asymmetric footprints cause directional and asymmetric radiation/reception patterns. The mismatches in these patterns as source and receiver positions change lead to variable source/receiver signatures. The non-stationarity of waveforms is made worse by transducer self-scattering and by scattering from the mounting hardware.

CONCLUSION

We recorded scale-modelled transmission seismograms across a 2D circular area within a homogeneous volume of water (“baseline” survey) using the piezoelectric buzzers mounted in the orientation shown on Figure 13(a). Plots of raw traces from an example CSG from the resulting dataset exhibit long-duration codas and non-stationarity. These two characteristics make the raw unprocessed traces poorly suited for efficient FWI imaging.

Before scale-modelled data acquired with buzzer transducer can be considered suitable for efficient FWI, we must make the source/receiver signatures recorded through the homogeneous water medium more nearly identical. Possibly, this can be done by changing the way the buzzers are mounted on the positioning gantries, so that the acquisition is done with the circular transducer footprints depicted on Figure A1(b).

We also must decrease the time-duration of the source wavelet codas, either by applying mechanical damping of some kind, or by numerically adjusting the HV signal driving the source transducer. Adjusting the HV signal driving the source transducer possibly can be accomplished by time-domain filtering (see Wong et al., this volume).

ACKNOWLEDGEMENT

We thank the sponsors of CREWES for continued support. This work was funded by CREWES industrial sponsors and NSERC (Natural Science and Engineering Research Council of Canada) through the grant CRDPJ 543578-19.

REFERENCES

Henley, D. C., 2021, Preliminary processing of physical modeling data from circular arrays, **33**, 15.

Pan, Wenyong, Kris Innanen, Gary Margrave, Scott Keating, 2015, Recover low-frequency for full-waveform inversion via band-limited impedance inversion and projection onto convex sets: CREWES Research Report, Vol. 27, no.60. https://www.crewes.org/Documents/ResearchReports/2015/CRR201560.pdf

Sirgue, L., and Pratt, R. G., 2004, Efficient waveform inversion and imaging: A strategy for selecting temporal frequencies: Geophysics, 69, 231–248.

Wong, Joe, Kevin W. Hall, Eric V. Gallant, Rolf Maier, Malcolm B. Bertram, and Don C. Lawton, 2009, Seismic Physical Modelling at the University of Calgary: CSEG Recorder, vol. 34, no.3. Mar 2009 | VOL. 34 No. 03 | View Issue

Wong, J., Henley, D. C., and Innanen, K. A. H., 2021, Analyzing buzzer-acquired physically-modelled data for FWI, **33**, 49.

APPENDIX: COMPARING BUZZER ORIENTATIONS

Buzzers can be mounted on the positioning motors of the Physical Modelling System in two ways. Figure A1 shows the transducer footprints in the XY plane for these alternatives. To this point in the present report, we have focused on results acquired with the mounting method that gives the footprint geometry of Figure A1(a). This Appendix briefly compares those results with results acquired with the alternative mounting method that gives the footprint geometry shown on Figure A1(b).

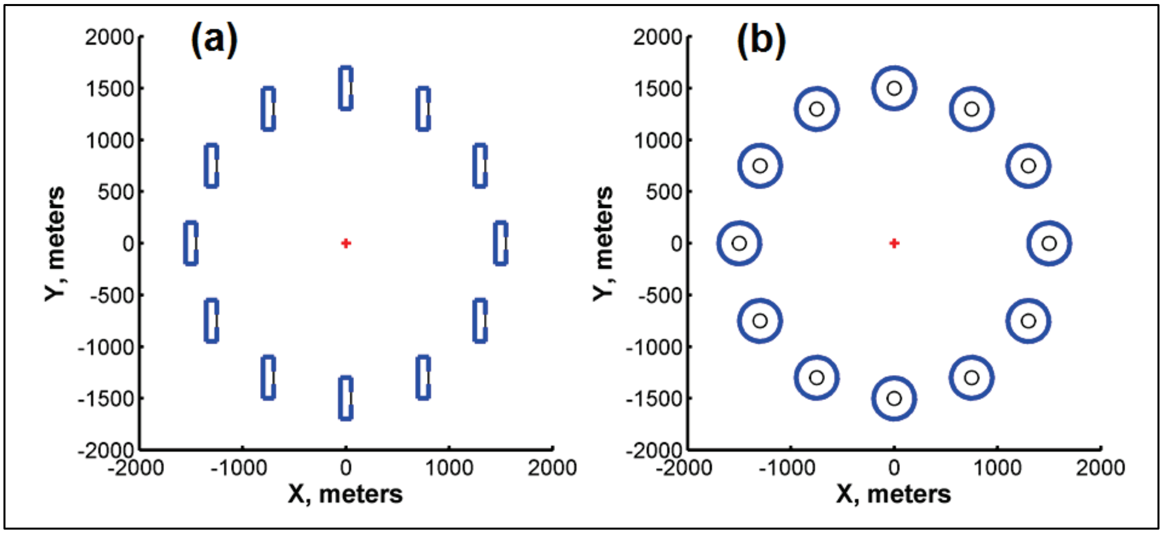

Fig A1: Plan views of two transducer orientations: (a) Rotation axes of buzzers pointing in the X-direction and ports facing to the right. (b) Rotation axes of buzzers pointing in the Z-direction and ports facing down.

Figure A2 displays CSG seismograms recorded with the first mounting alternative for which the transducer footprints in the XY plane are rectangular. The waveforms are not uniform but change as the receiver position changes. In this case, because the transducers are not radially symmetric in the XY plane, individual transducer radiation/reception patterns are also not radially symmetric. The long-duration vibrations (produced and sensed by the buzzers in damped resonance) and the mismatch in the radiation and reception patterns as the source remains fixed while the receiver changes position are the reasons for the non-stationarity of the recorded waveforms. Asymmetric self-scattering from the transducers contributes to the non-stationarity.

The second mounting method gives the circular transducer footprints shown on Figure A1(b). In this orientation, the radiation/reception patterns should be radially symmetric relative to the transducer centers, as also should be the self-scattering. Therefore, in a homogeneous medium, the waveforms of seismograms acquired using this mounting method should be more uniform as receiver positions change.

Figures A2 and A3 are plot of trace-normalized seismograms for an example CSG acquired with rectangular and circular transducer footprints, respectively. A visual comparison shows that the seismograms recorded with the circular footprints are more consistent and uniform. However, the resonance effects are less damped, causing the stronger amplitudes at late times.

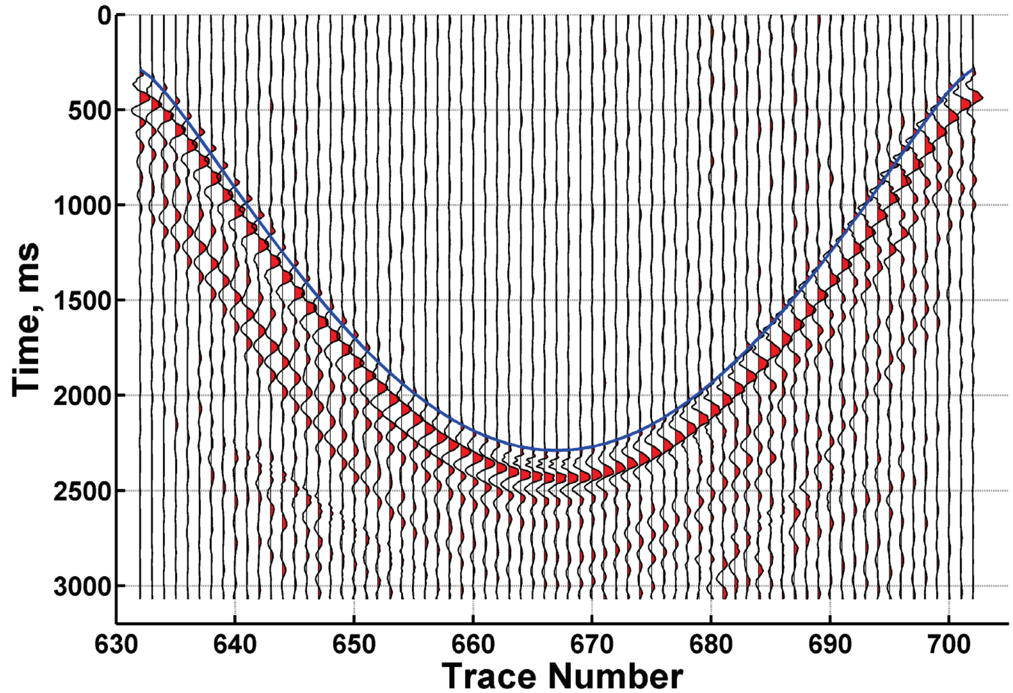

Fig A2: Trace-normalized display of common-source seismograms acquired with transducers mounted so that their footprints are rectangular in the XY plane.

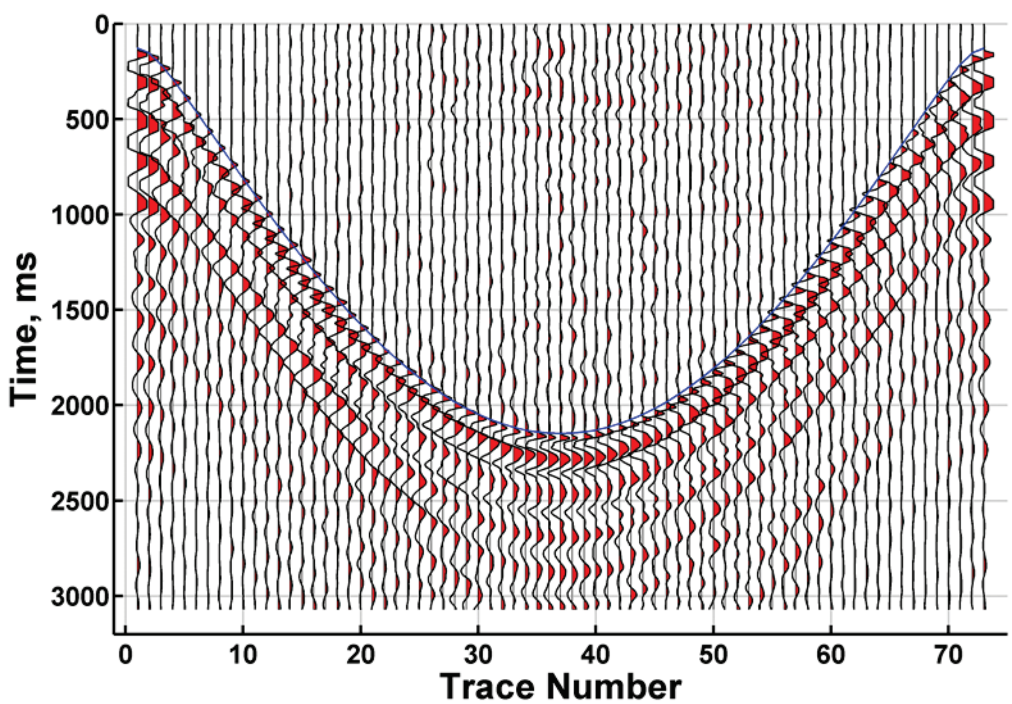

Fig A3: Trace-normalized display of common-source seismograms acquired with transducers mounted so that their footprints are circular in the XY plane.

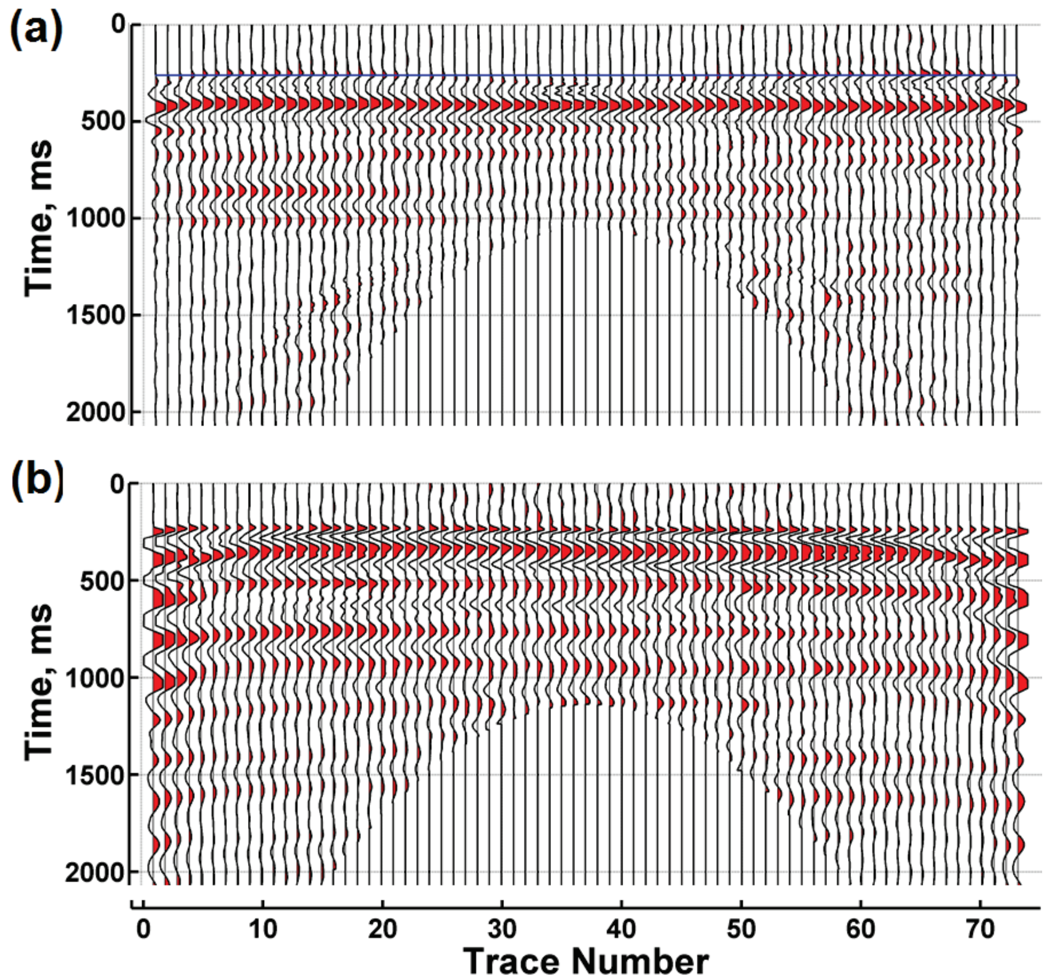

Fig. A4. Trace-normalized display of common-source seismograms (a) acquired with rectangular transducer footprints; (b) with circular transducer footprints. No other processing.

Figure A4 plots the flattened versions of the above CSGs. Flattening facilitates the comparison of the waveforms recorded with the two alternative footprints of buzzers in the XY plane. The figure shows that, for times less than about 500ms, the aligned traces acquired with the rectangular footprints are more uniform than those acquired with the circular footprints. For times greater than 500ms, the traces acquired with the circular footprints are more uniform. However, traces recorded with the circular footprints have longer codas due to under-damping of resonance effects within the buzzer transducers.

Based on the evidence shown on Figure A4, it cannot be decide which of the two mounting methods is preferable. If we are able to significantly reduce the long-duration resonance effects using some sort of mechanical damping, then arguments emphasizing geometric symmetry would force the decision in favor of mounting to give circular footprints.